Generalized Langevin Equation

Stochastic Differential Equations

Sankarasubramanian Ragunathan

389851

RWTH Aachen University

Agenda

Scope of the Project

What? Generalized Langevin Dynamics is a modeling technique that can be used to model anomalous diffusive phenomena observed in viscoelastic fluids.

Why? GLE succeeds in capturing sub-diffusive and super-diffusive behavior. But GLE is *Non-Markovian* i.e. `memory kernel` depends on the history of velocity. This issue is overcome by using Extended Variable GLE that considers a finite dimensional subspace for the `memory kernel`.

How? Study Extended Variable GLE using Prony series approximation. Accuracy of Explicit Euler and Splitting Numerical schemes are also tested to find out the "optimal scheme". Study local and global sensitivity of the observables to perturbations of the extended variable GLE.

Where? Applications of GLE include but are not restricted to micro-rheology, biological systems, nuclear quantum effects and systems in which anomalous diffusion arise.

Langevin dynamics as a computational tool

What? **Langevin Dynamics:** Large particles in a bath of small particles, motion of large particles directly integrated while the dynamics of small particles are "averaged out".

Why? *Molecular Dynamics* simulations involving all particles is computationally expensive. Langevin Equation model is computationally cheaper.

Drawback

Anomalous diffusion problems arising due to *Power Law* behavior of solute-solvent systems cannot be solved.

Solution

Generalized Langevin Equation (**GLE**)

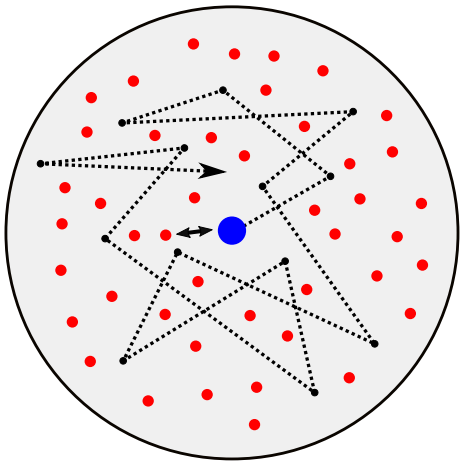

(a) Big Particles interacting with Smaller Particles

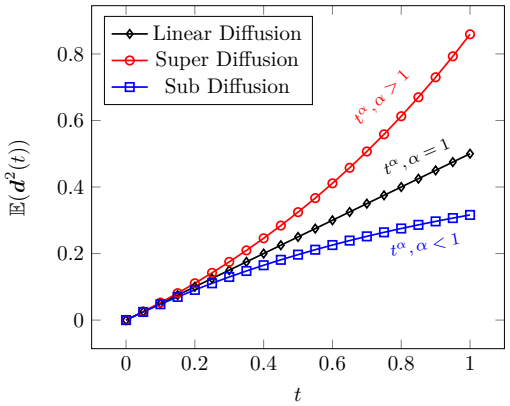

(b) Sub-diffusive and Super-diffusive behavior of solute-solvent systems

Mathematical Model for Anomalous Diffusion

The velocity term of GLE is based on *Ornstein-Uhlenbeck* process.

GLE Equations

$$d\boldsymbol{X}(t) = \boldsymbol{V}(t)dt \tag{1}$$

$$M d\boldsymbol{V}(t) = \underbrace{\boldsymbol{F}^c(\boldsymbol{X}(t))dt}_{\substack{\text{Conservative Force due to Potential}}} \underbrace{- \int_0^t \boldsymbol{\Gamma}(t-s)\boldsymbol{V}(s)dsdt}_{\substack{\text{Temporally Non-Local Drag } \left(\boldsymbol{F}^d\right) \text{ Force}}} + \underbrace{\boldsymbol{F}^r(t)dt}_{\substack{\text{Random Correlated Force given by } FDT}} \tag{2}$$

$$\boldsymbol{X}(0) = \boldsymbol{X}_0, \quad \boldsymbol{V}(0) = \boldsymbol{V}_0 \quad \text{(Initial Conditions)} \tag{3}$$

Note:

$\boldsymbol{F}^r$ and $\boldsymbol{F}^d$ are characterized by the `memory kernel` consistent with **FDT**.

Mathematical Model for Anomalous Diffusion

Theorem

FDT (Fluctuation Dissipation Theorem) states that the equilibration to a temperature, T, requires that the two-time correlation of $\boldsymbol{F}^r(t)$ and $\boldsymbol{\Gamma}(t)$ be related as:

$$\left\langle \boldsymbol{F}_i^r(t+s), \boldsymbol{F}_j^r(t) \right\rangle = k_B T \boldsymbol{\Gamma}(s) \delta_{ij}, \qquad s \geq 0 \tag{4}$$

where k_B is the Boltzmann's Constant, δ_{ij} is the Kronecker Delta and i,j represent distinguished non-interacting particles (in our case, the solute particles that we are modeling). Hence FDT correlates the random forces for a given solute particle at different times.

Note:

- $\boldsymbol{F}^d(t)$ depends on the velocity history unlike in *Langevin Equation* where it depends on the velocity at that instant.
- The random forces are not just delta correlated but are correlated by the `memory kernel`. `Memory Kernel` choice and approximation important based on the problem to be studied.

Complications due to memory effects

Complications

1. Storage of subset of the time history of $\boldsymbol{V}(t)$.
2. Sequence of $\boldsymbol{F}^r(t)$ given by `FDT`.
3. Numerical SDE solution should converge in distribution.

Solution

1. Using extended variable `Prony Series` for `Memory Kernel`.

$$\boldsymbol{\Gamma}(t) \approx \sum_{k=1}^{N_k} \frac{c_k}{\tau_k} \exp\left[-\frac{t}{\tau_k}\right], \qquad t \geq 0 \tag{5}$$

   where N_k is the number of terms used in approximating the `memory kernel`.

2. Using a suitable integration scheme for the numerical method.

Complications due to memory effects

Why use extended variable Prony Series?

- Approximation of `memory kernel` to map **Non-Markovian** GLE to **Markovian** system of N_k variables.
- Typically used for modelling *Power Law* based decay/growth as observed in sub/super diffusive systems.

Importance of choice of integration scheme?

- Conservation of moments of variables of interest such as displacement and velocity (usual variables of interest for MD simulations)
- Convergence of **GLE** to Langevin equation in the limit of small τ_k as observed in theory.

Note: In the numerical experiments carried out in this presentation, we consider sub-diffusive decaying behavior which behaves as $t^{-\alpha}$ where $\alpha < 1$ and hence we use a decaying Prony series to approximate the memory function.

Extended Variable GLE formulation

Main Extended Variable GLE Equations

$$m_i dV_i(t) = F_i^c(\boldsymbol{X}(t))dt + \sum_{k=1}^{N_k} S_{i,k}\,dt \tag{6}$$

$$dX_i(t) = V_i(t)dt \tag{7}$$

$$dS_{i,k}(t) = -\frac{1}{\tau_k} S_{i,k}(t)dt - \frac{c_k}{\tau_k} V_i(t)dt + \frac{1}{\tau_k}\sqrt{2k_B T c_k}\,dW_{i,k}(t) \tag{8}$$

Auxiliary Extended Variable GLE Equations

$$S_{i,k}(t) = Z_{i,k}(t) + F_{i,k}(t) \tag{9}$$

$$dZ_{i,k}(t) = -\frac{1}{\tau_k} Z_{i,k}(t)dt - \frac{c_k}{\tau_k} V_i(t)dt \qquad Z_{i,k}(t) = -\int_0^t \frac{c_k}{\tau_k}\exp\left[-\frac{(t-s)}{\tau_k}\right] V_i(s)ds \tag{10}$$

$$dF_{i,k}(t) = -\frac{1}{\tau_k} F_{i,k}(t)dt + \frac{1}{\tau_k}\sqrt{2k_B T c_k}\,dW_{i,k}(t) \qquad \left\langle F_{i,k}(t+s), F_{i,k}(t)\right\rangle = k_B T \frac{c_k}{\tau_k}\exp\left[-\frac{s}{\tau_k}\right] \tag{11}$$

$$F_i^r(t) = \sum_{k=1}^{N_k} F_{i,k}(t) \tag{12}$$

Explicit Euler vs. Splitting Schemes

Numerical Schemes:

- Explicit Euler Scheme.
- Splitting Scheme.

Which numerical scheme to choose for solving the problem?

General observables/physical quantities that are measured to understand the behavior of a system. E.g., *Mean Square Displacement* (`MSD`) and *Velocity Autocorrelation Function* `VAF` in microrheology. Therefore essential to consider scheme that conserves the first and second moments of $\boldsymbol{V}(t)$ and $\boldsymbol{X}(t)$ for validating the simulations.

Implementation Details:

- Uniform time-step size, Δt, where $N_t \Delta t = T_{\text{tot}}$ (T_{tot} represents the total time of the simulation and N_t represents the # of time-steps.)
- All N_p particles are seeded with the same constant $\boldsymbol{X}(0)$ and $\boldsymbol{V}(0)$ (**Note:** We could also seed the initial conditions based on *Boltzmann* distribution.)
- The composite variable $S_{i,k}(t)$ is assumed to be zero initially.

Explicit Euler vs. Splitting Schemes

Explicit Euler Scheme

Input: $\boldsymbol{X}(0), \boldsymbol{V}(0), \boldsymbol{S}(0)$
Output: $\boldsymbol{X}(t), \boldsymbol{V}(t)$

1: **for** $n = 0$ to N_t **do**
2: $V_i^{n+1} = V_i^n + \frac{\Delta t}{m_i} F_i^c\left(\boldsymbol{X}^n\right) + \frac{\Delta t}{m_i} \sum_{k=1}^{N_k} S_{i,k}^n$ ▷ Advance $\boldsymbol{V}(t)$ by a full step
3: $X_i^{n+1} = X_i^n + \Delta t V_i^n$ ▷ Advance $\boldsymbol{X}(t)$ by a full step
4: $S_{i,k}^{n+1} = \left(1 - \frac{\Delta t}{\tau_k}\right) S_{i,k}^n - \frac{c_k \Delta t}{\tau_k} V_i^n + \frac{1}{\tau_k} \sqrt{2 \mathrm{k_B} T c_k} \Delta W_{i,k}$ ▷ Advance $\boldsymbol{S}(t)$ by a full step
5: **end for**

Splitting Scheme

Input: $\boldsymbol{X}(0), \boldsymbol{V}(0), \boldsymbol{S}(0)$
Output: $\boldsymbol{X}(t), \boldsymbol{V}(t)$

1: **for** $n = 0$ to N_t **do**
2: $V_i^{n+1/2} = V_i^n + \frac{\Delta t}{2m_i} F_i^c\left(\boldsymbol{X}^n\right) + \frac{\Delta t}{2m_i} \sum_{k=1}^{N_k} S_{i,k}^n$ ▷ Advance $\boldsymbol{V}(t)$ by a half step
3: $X_i^{n+1} = X_i^n + \Delta t V_i^{n+1/2}$ ▷ Advance $\boldsymbol{X}(t)$ by a full step
4: $S_{i,k}^{n+1} = \theta_k S_{i,k}^n - (1 - \theta_k) c_k V_i^{n+1/2} + \alpha_k \sqrt{2 \mathrm{k_B} T c_k} \Delta W_{i,k}$ ▷ Advance $\boldsymbol{S}(t)$ by a full step
5: $V_i^{n+1} = V_i^{n+1/2} + \frac{\Delta t}{2m_i} F_i^c\left(\boldsymbol{X}^{n+1}\right) + \frac{\Delta t}{2m_i} \sum_{k=1}^{N_k} S_{i,k}^{n+1}$ ▷ Advance $\boldsymbol{V}(t)$ by a half step
6: **end for**

Explicit Euler vs. Splitting Schemes - Case Study

Assumptions:

- One dimensional problem, $d = 1$
- Single mode in the Prony series approximation, $N_k = 1$
- Zero conservative force acting on the particles, $\boldsymbol{F}^c\left(\boldsymbol{X}(t)\right) = 0$

The case study is simulated using both numerical schemes, *Explicit Euler* and *Splitting Method*, for three different τ and c values in the `Prony Series` approximation (Table 1)

Type of System	c	τ
Under-damped	1	1
Critically-damped	0.5	0.5
Over-damped	0.25	0.25

Table: c and τ values used for the case study

Explicit Euler vs. Splitting Schemes - Results

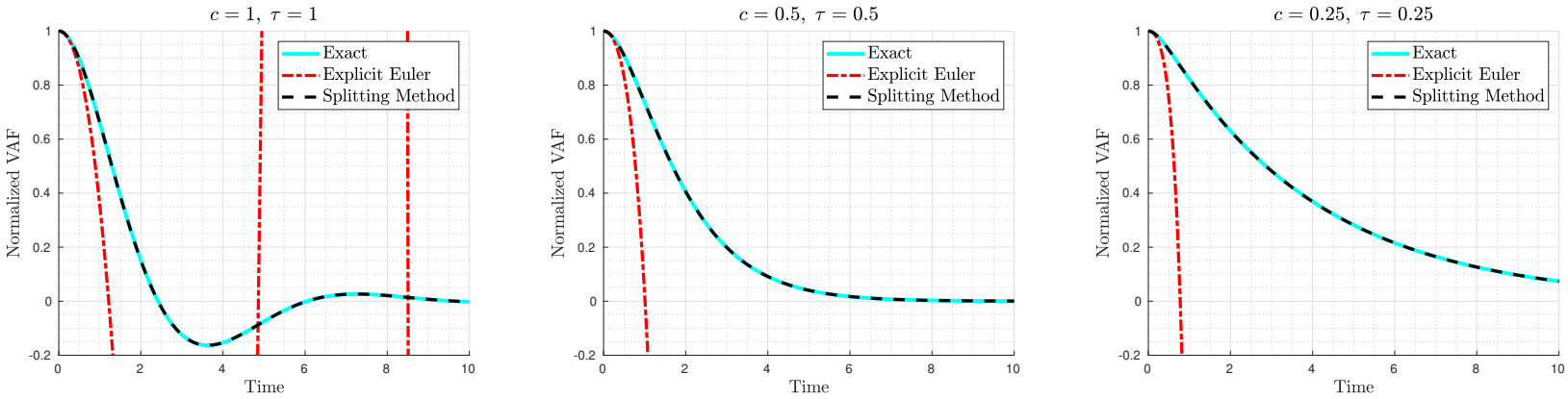

(a) Under-damped **(b)** Critically-damped **(c)** Over-damped

Figure: Normalized VAF vs. Time for Explicit Euler and Splitting schemes($\delta t = 0.01, N_p = 1000, N_k = 1$)

Normalized VAF (*Velocity Autocorrelation Function*)

$$\frac{\langle \boldsymbol{V}(t), \boldsymbol{V}(0) \rangle}{\langle \boldsymbol{V}(0), \boldsymbol{V}(0) \rangle} = \begin{cases} \exp\left[-\frac{t}{2\tau}\right]\left(\cos\left(\Omega t\right) + \frac{1}{2\tau\Omega}\sin\left(\Omega t\right)\right) & \text{for } \Omega \neq 0 \\ \exp\left[-\frac{t}{2\tau}\right]\left(1 + \frac{t}{2\tau}\right) & \text{for } \Omega = 0 \end{cases} \tag{13}$$

$$\Omega = \sqrt{c/\tau - 1/4\tau^2}$$

Note: One mode Prony series approx. without any conservative force terms.

Explicit Euler vs. Splitting Schemes - Results

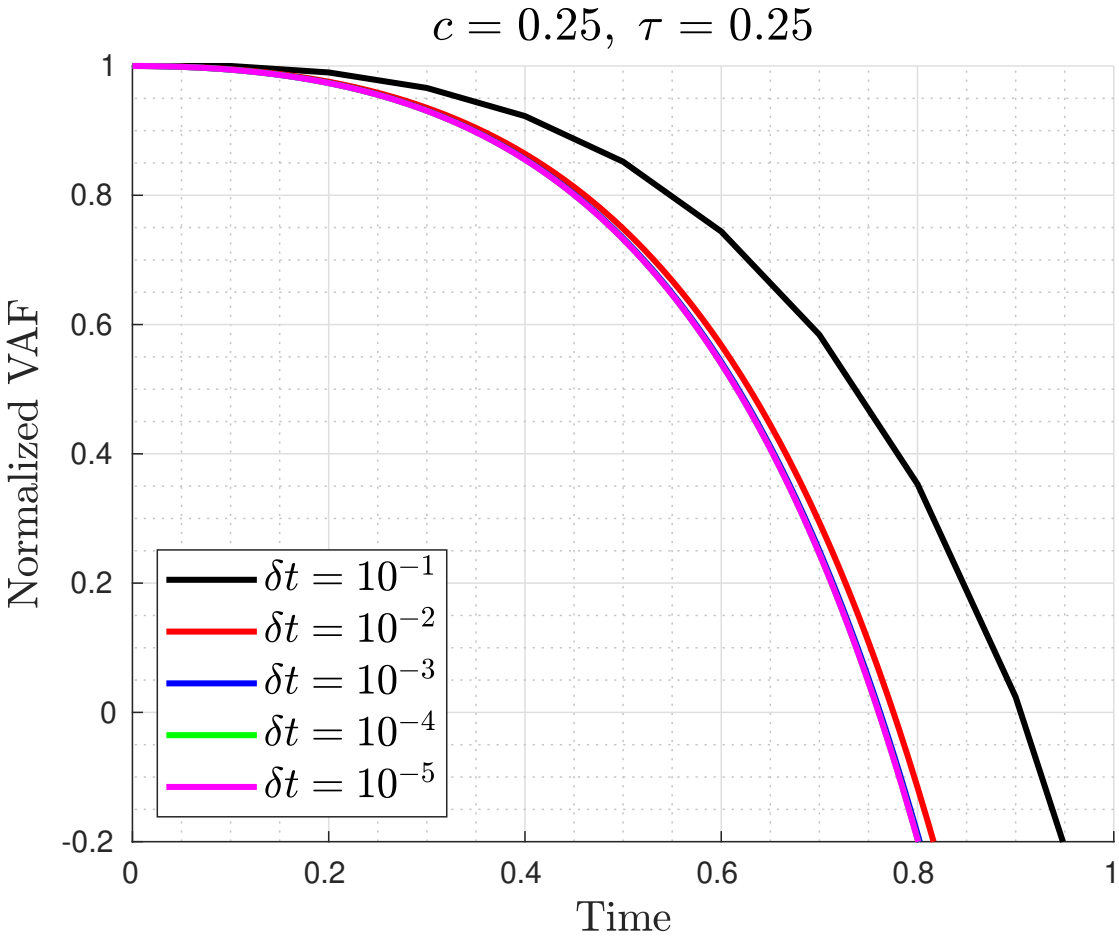

Figure: Normalized VAF vs. Time for Explicit Euler scheme for different time step sizes. Here we have considered zero conservative force acting on the particles with one mode Prony series approximation. We can see that even on using very fine time-step size, the Explicit Euler scheme does not conserve moments.

First and Second moment conserving Splitting schemes

Observation: Explicit Euler scheme produces wrong results for the `Normalized VAF` as when compared to the Splitting scheme (***Reason:*** *Independent updates for* $\boldsymbol{X}(t)$ *and* $\boldsymbol{V}(t)$ *when using Explicit Euler scheme.*)

Solution: Using the Splitting scheme as the preferred integration scheme for all proceeding numerical experiments and sensitivity analysis studies.

Harmonic Potential Well - Problem

Harmonic Potential Well GLE

$$d\boldsymbol{V}(t) = \underbrace{-\omega_0^2 \boldsymbol{X}(t)}_{\substack{\text{Conservative Force arising from Harmonic Potential}}} dt - \underbrace{\int_0^t \frac{\gamma_\lambda}{\Gamma_0\,(1-\lambda)}\,(t-s)^{-\lambda}\,\boldsymbol{V}(s)dsdt}_{\substack{\textit{Power Law decay memory kernel function}}} + \boldsymbol{M}^{-1}\boldsymbol{F}^r(t)dt \tag{14}$$

Question?

Approximation of the `memory kernel` in Equation (14) using Prony series

Answer:

log-spaced values for τ_k from $\Delta t/10$ to $10N_t\Delta t$ and then linearly fitting c_k using *least squares regression* i.e.

$$\min_{\boldsymbol{x}} ||\boldsymbol{A}\cdot\boldsymbol{x}-\boldsymbol{b}||^2, \quad \boldsymbol{x}=\{c_k\} \quad \forall k=1,\cdots,N_k$$

Harmonic Potential Well - Parameter Fitting

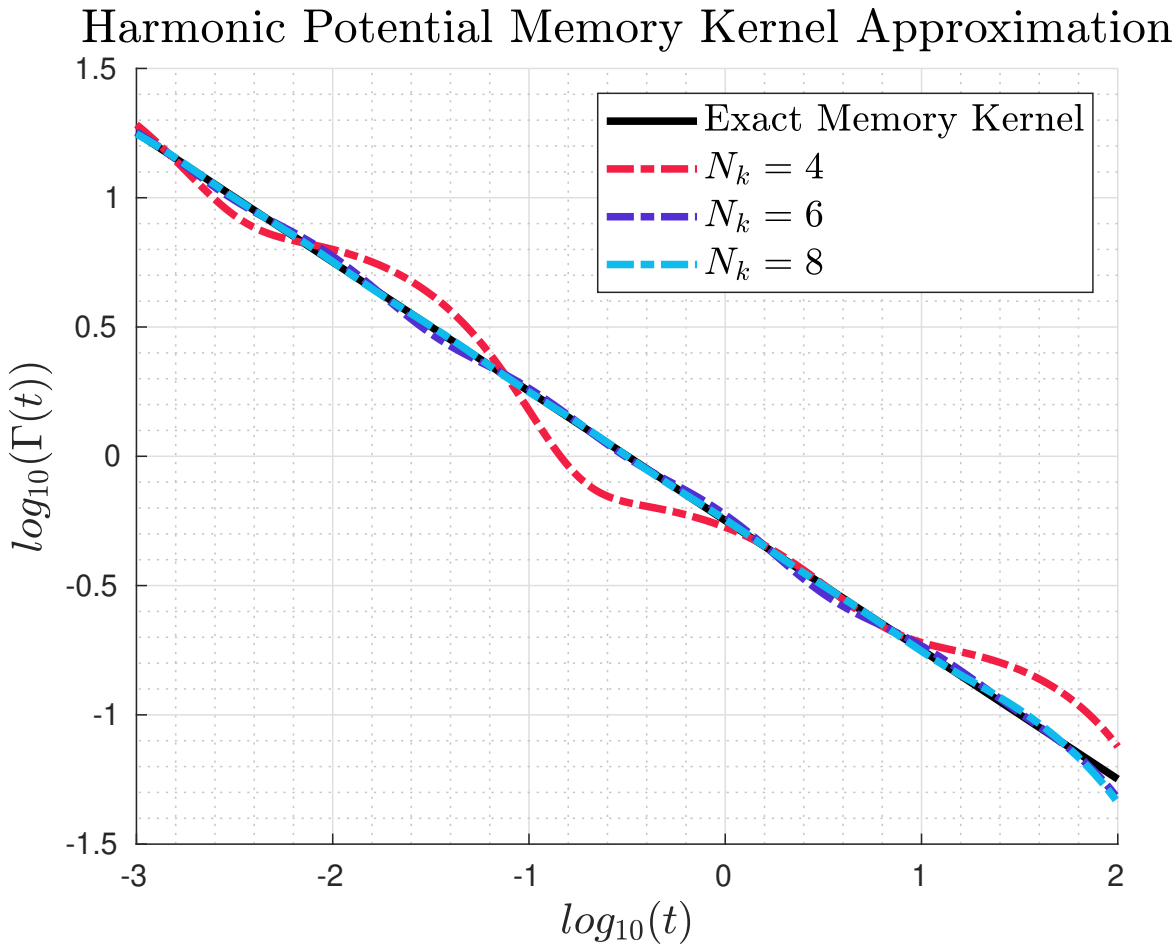

Figure: A Prony series fit of the *power law* memory kernel in eq. (14) for $\gamma_\lambda = 1$, $\lambda = 0.5$ for different N_k

Harmonic Potential Well - Normalized VAF & Pointwise Error

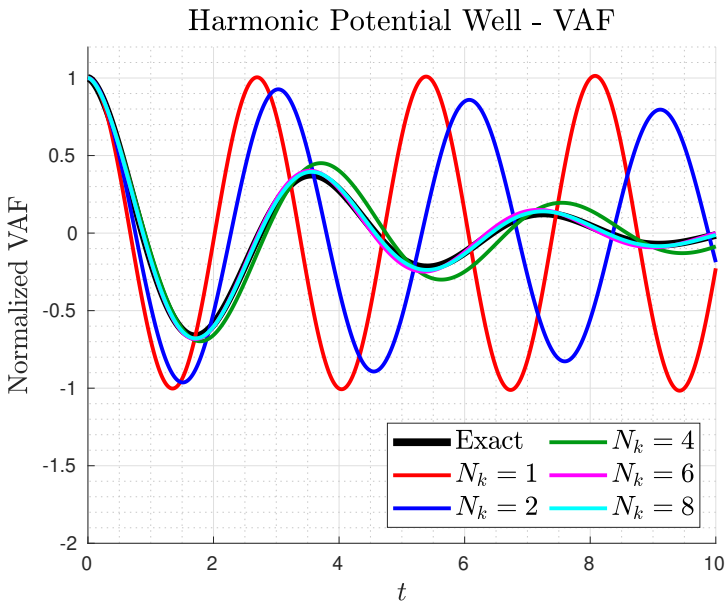

(a) Normalized VAF at different times for different no. of modes used in Prony series approximation

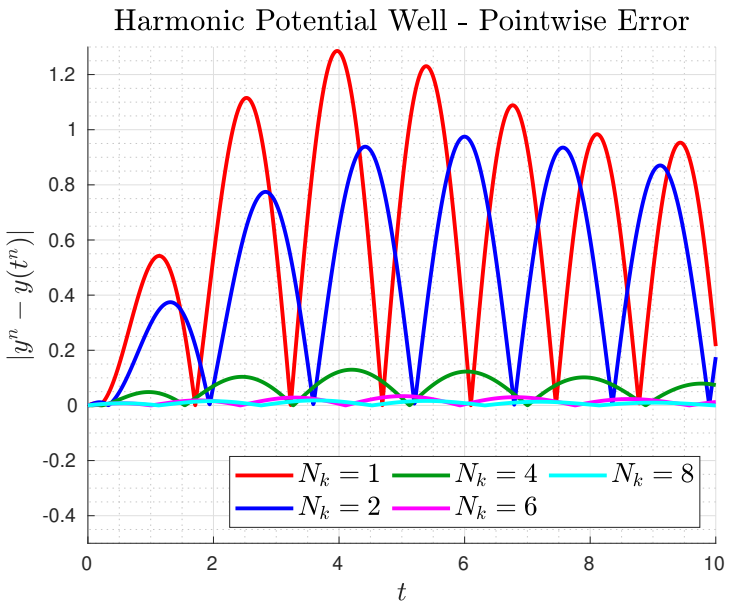

(b) Pointwise error in VAF at different times for different no. of modes used in Prony series approximation

Figure: Approximation of the Harmonic Potential Well problem for $\gamma_\lambda = 1$, $\lambda = 0.5$ and $\omega_0 = 1.4$ using Prony series approximation

Harmonic Potential Well - Normalized VAF & Pointwise Error

Normalized VAF - Exact Solution

$$\underbrace{C_V(t)}_{\text{Normalized VACF}} = \sum_{k=0}^{\infty} \frac{(-1)^k}{k!} (\omega_0 t)^{2k} \, \mathscr{E}^{(k)}_{2-\lambda,1+\lambda k} \left(-\gamma_\lambda t^{2-\lambda}\right)$$

where $\mathscr{E}^{(k)}_{\alpha,\beta}(y)$ represents the k$^{\text{th}}$ derivative of the *Generalized Mittag-Leffler* function given by:

$$\mathscr{E}^{(k)}_{\alpha,\beta}(y) = \sum_{j=0}^{\infty} \frac{(j+k)!\, y^j}{j!\, \Gamma_0\left(\alpha(j+k)+\beta\right)}$$

Harmonic Potential Well - Normalized MSD

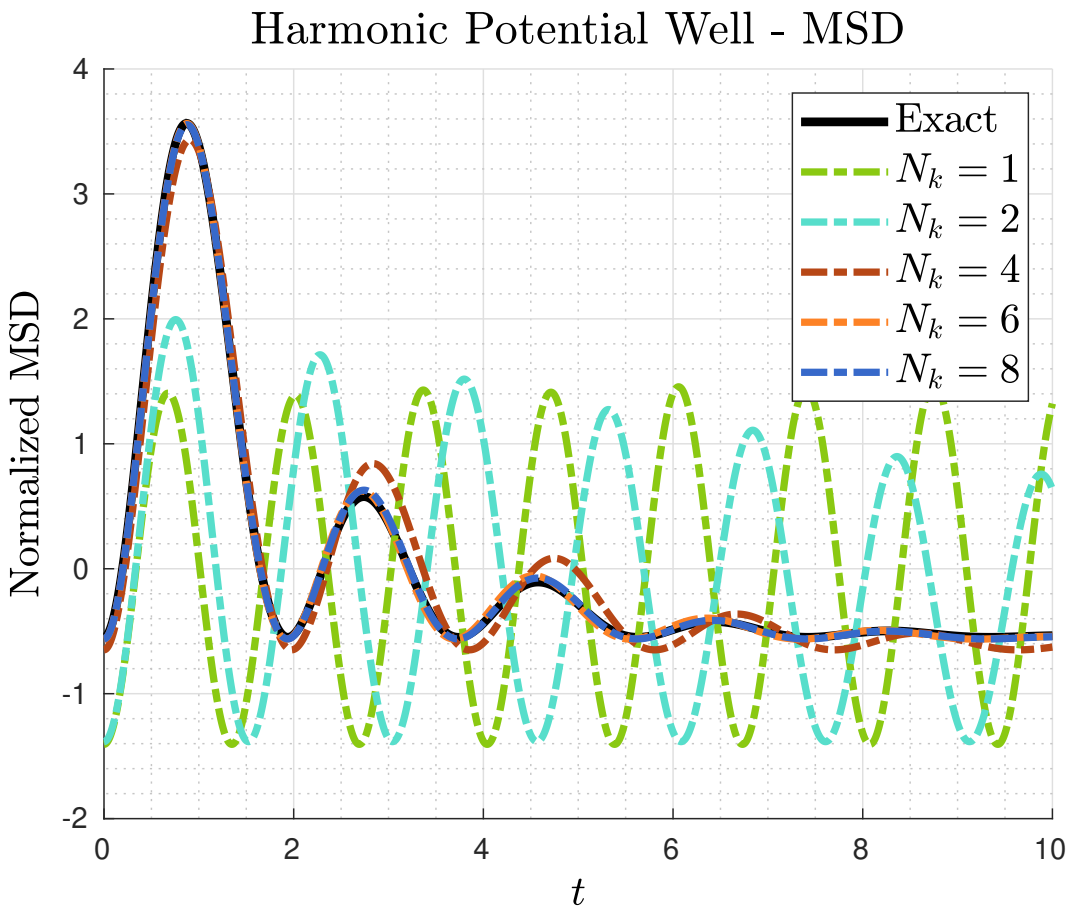

Figure: Normalized MSD at different times for different no. of modes used in Prony series approximation. ($\gamma_\lambda = 1$, $\lambda = 0.5$ and $\omega_0 = 1.4$)

Harmonic Potential Well - Normalized MSD

Normalized MSD - Exact Solution

$$\underbrace{\left\langle [\boldsymbol{X}(t+\tau)-\boldsymbol{X}(t)]^2 \right\rangle}_{\text{Normalized MSD}} = \frac{2\mathsf{k}_\mathsf{B}T}{m} I(\tau) - 2x_0 v_0 \omega_0^2 \left[G(t+\tau)-G(t)\right]\left[I(t+\tau)-I(t)\right]$$
$$+ \left(v_0^2 - \frac{\mathsf{k}_\mathsf{B}T}{m}\right)\left[G(t+\tau)-G(t)\right]^2$$
$$+ \omega_0^2 \left(x_0^2\omega_0^2 - \frac{\mathsf{k}_\mathsf{B}T}{m}\right)\left[I(t+\tau)-I(t)\right]^2$$

$$I(t) = \sum_{k=0}^{\infty} \frac{(-1)^k}{k!} \omega_0^{2k} t^{2(k+1)} \mathscr{E}^{(k)}_{2-\lambda,3+\lambda k}\left(-\gamma_\lambda t^{2-\lambda}\right) \qquad \text{(Kernel integral)}$$

$$G(t) = \sum_{k=0}^{\infty} \frac{(-1)^k}{k!} \omega_0^{2k} t^{2k+1} \mathscr{E}^{k}_{2-\lambda,2+\lambda k}\left(-\gamma_\lambda t^{2-\lambda}\right) \qquad \text{(Relaxation function)}$$

where v_0,x_0 represent the velocity and position of the particles at time $t = 0$.

Harmonic Potential Well - Normalized PAF

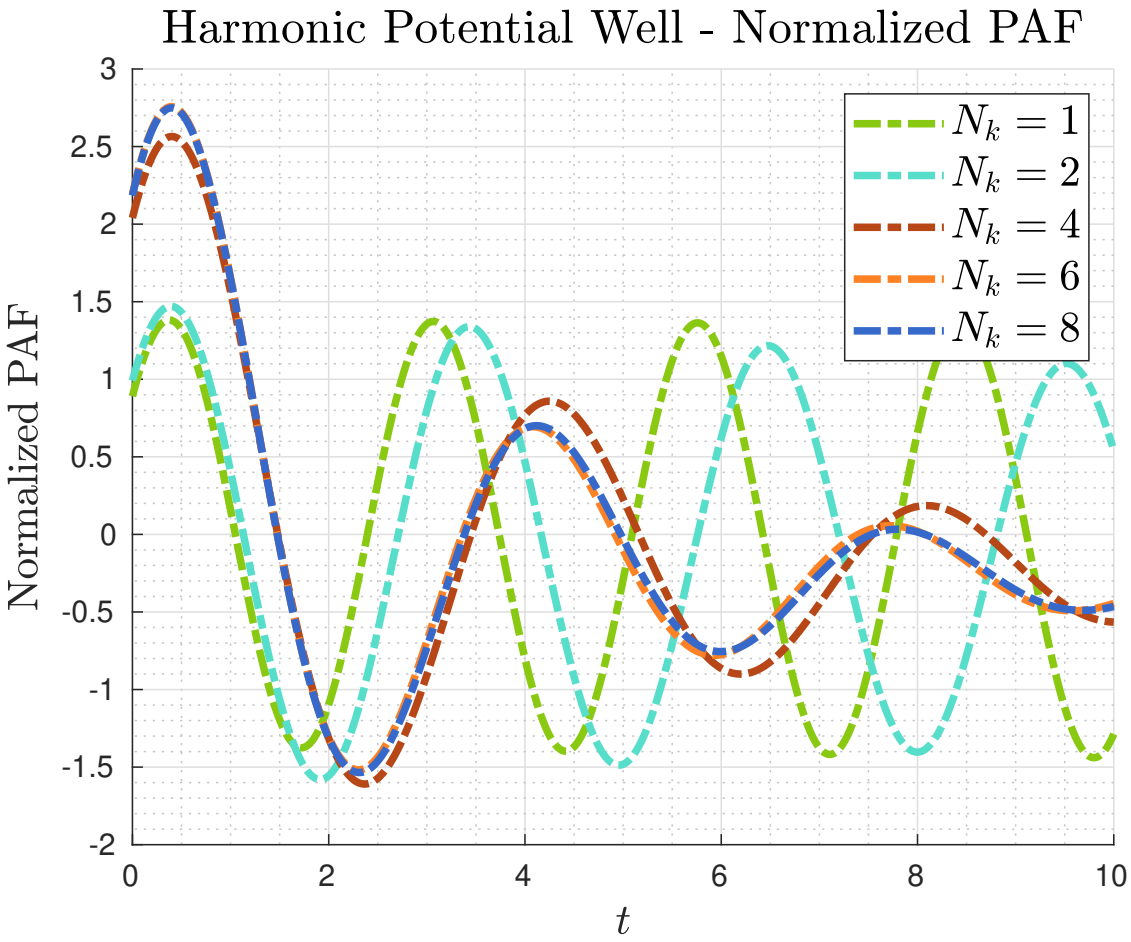

Figure: Normalized PAF, $\frac{\langle \boldsymbol{X}(t), \boldsymbol{X}(0) \rangle}{\langle \boldsymbol{X}(0), \boldsymbol{X}(0) \rangle}$ vs. Time for Harmonic Potential Well problem when approximated with varying no. of terms in the Prony series approximation ($\gamma_\lambda = 1$, $\lambda = 0.5$ and $\omega_0 = 1.4$)

Need for Sensitivity Analysis

Question?

Why do we need to perform global and local sensitivity analysis?

Answer:

- Extended variable GLE fitted by matching `MSD` or `VAF` obtained from experimental data. Prony series parameters c_k, τ_k, N_k sensitive to experimental data i.e. to errors in measurement or lack of data. Also determine N_k such that the error in the fit is lower than certain tolerance.
- *Ergodicity breaking:* Time averaged statistics such as `MSD` do not converge to ensemble averages i.e. there is a large "spread" (variance) in the observables.

Mathematical Tools for Local Sensitivity Analysis

Sensitivity Analysis

Let $\mathcal{S}(t, \theta; f)$ denote the sensitivity of the stochastic process $\boldsymbol{X}_t(\theta)$ where θ is a parameter that affects the stochastic process and f is the given observable. We are interested in calculating:

$$\mathcal{S}(t, \theta; f) = \frac{\partial \mathbb{E}\left[f\left(\boldsymbol{X}_t(\theta)\right)\right]}{\partial \theta}$$

Methods of Calculation:

- *Finite Difference Stencils:* Approximating derivative by a finite difference stencil and obtain the required moments by Monte Carlo.
- *Likelihood Ratio:* Expressing sensitivity as an expectation of f under a change of measure.
- *Malliavin Calculus:* Extension of calculus of variations to stochastic processes.

Mathematical Tools for Local Sensitivity Analysis

Finite Difference Stencil

$$\mathcal{S}_{\varepsilon}\left(t,\theta;f\right)=\frac{\mathbb{E}\left[f\left(\boldsymbol{X}_{t}\left(\theta+\varepsilon\right)\right)\right]-\mathbb{E}\left[f\left(\boldsymbol{X}_{t}\left(\theta\right)\right)\right]}{\varepsilon}$$

Likelihood Estimator

$$\begin{aligned}\mathcal{S}_{LR}\left(t,\theta;f\right)=\frac{\partial\mathbb{E}\left[f\left(\boldsymbol{X}_{t}\left(\theta\right)\right)\right]}{\partial\theta}&=\int f\left(x_{t}\right)\left[\partial_{\theta}\log g\left(\theta,x_{t}\right)\right]g\left(\theta,x_{t}\right)dx_{t}\\&=\mathbb{E}\left[f\left(\boldsymbol{X}_{t}\left(\theta\right)\right)\partial_{\theta}\log g\left(\theta,\boldsymbol{X}_{t}\right)\right]\end{aligned}$$

where g represents the change in measure by a p.d.f. g is unknown which means that it is difficult to calculate local sensitivity using likelihood estimator. Also there is no appropriate change of measure on path space as the parameters c_k and τ_k appear in both drift and diffusion terms.

Malliavin Calculus

$$\mathcal{S}_{M}\left(t,\theta;f\right)=\mathbb{E}\left[f\left(\boldsymbol{X}_{T}\right)h\left(\left\{\boldsymbol{X}_{s}\right\}_{0\leq s\leq T}\right)\right]$$

where $h\left(.\right)$ represents the Malliavin weights that are non-unique. $h(.)$ is difficult to calculate as it involves solving a system of auxiliary processes obtained using Malliavin Calculus.

Efficient Local Sensitivity Analysis using FD Stencils for Coupled Random Path

Objective: To find a reduced variance sampling strategy for calculating the local sensitivity.

Methodology: Let $\hat{\phi}(\theta)$ represent the expected value of the observable $f(\boldsymbol{X}_t(\theta))$. Then we can write,

$$\hat{\phi}(\theta) = M^{-1}\sum_{i=1}^{M} f(X_{i,t}(\theta)) \Rightarrow \mathcal{S}_\varepsilon\left(t,\theta;\hat{\phi}\right) \approx \Delta_c(M,\varepsilon) = \frac{\hat{\phi}(\theta+\varepsilon)-\hat{\phi}(\theta-\varepsilon)}{2\varepsilon}$$

where each random variable is sampled independently of each other.

$$\Rightarrow \mathrm{Var}[\Delta_c] = \varepsilon^{-2}\mathrm{Var}\left[\hat{\phi}(\theta+\varepsilon)-\hat{\phi}(\theta-\varepsilon)\right]$$

$$= \varepsilon^{-2}M^{-1}\mathrm{Var}\left[\underbrace{f(\boldsymbol{X}_t(\theta+\varepsilon))}_{R_1} - \underbrace{f(\boldsymbol{X}_t(\theta-\varepsilon))}_{R_2}\right]$$

where the variance can be rewritten as

$$\mathrm{Var}[\Delta_c] = \varepsilon^{-2}M^{-1}\left(\mathrm{Var}[R_1]+\mathrm{Var}[R_2]-2\mathrm{Cov}[R_1,R_2]\right)$$

Efficient Local Sensitivity Analysis using FD Stencils for Coupled Random Path

Statistical Error is given by $\epsilon_M = \frac{C_\alpha \sigma}{\sqrt{M}}$ where $\sigma = \sqrt{\text{Var}\left[\Delta_c\right]}$ and C_α is a constant based on the confidence level of the solution

Coupled vs. Decoupled Noise:

- If R_1 and R_2 are not correlated, then $\text{Var}\left[\Delta_c\right] = \mathcal{O}\left(\varepsilon^{-2} M^{-1}\right)$
- If R_1 and R_2 are positively correlated, then $\text{Var}\left[\Delta_c\right] = \mathcal{O}\left(M^{-1}\right)$

Observation:

Let $\varepsilon = 0.1$. In order to reduce the error by a factor of 10.

- *Coupled Noise:* $M = 10^2$ samples
- *Decoupled Noise:* $M = 10^4$ samples

Hence the statistical error becomes independent of the perturbation parameter on using a common random path coupling i.e. R_1 and R_2 use the same Wiener process dW.

Local Sensitivity Analysis - Coupled vs. Decoupled Random Path

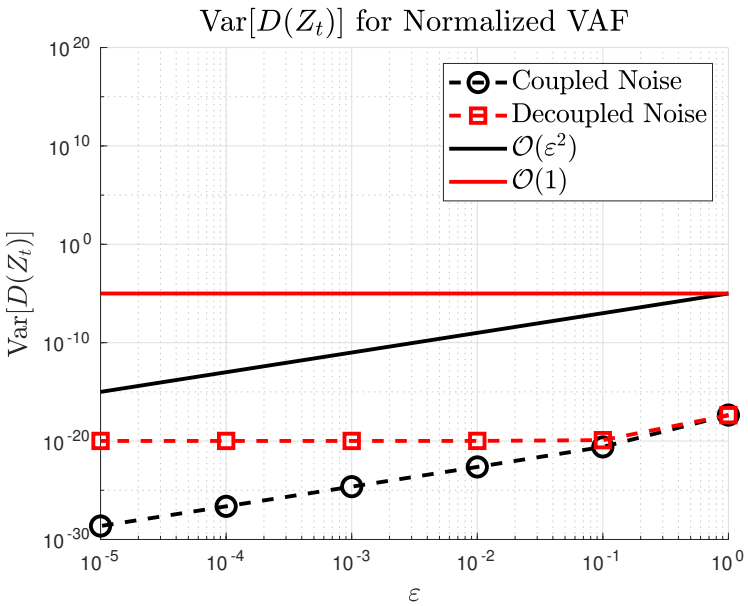

(a) Var $[D(Z_t)]$ for Normalized VAF where $D(Z_t) = \left(\hat{f}(\theta+\varepsilon) - \hat{f}(\theta-\varepsilon)\right)$

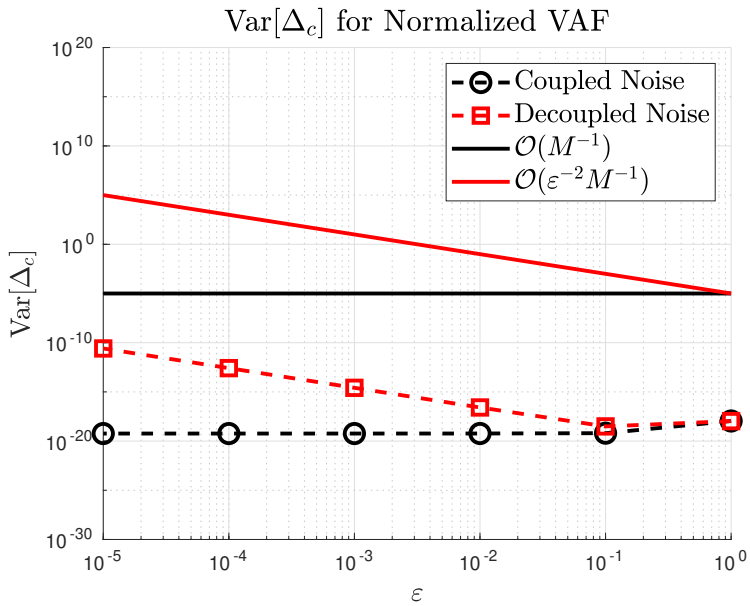

(b) Var $[\Delta_c]$ for Normalized VAF where $\Delta_c = \left(\hat{\phi}(\theta+\varepsilon) - \hat{\phi}(\theta-\varepsilon)\right)/2\varepsilon$

Figure: Order of variance reduction when using *Coupled* vs. *Decoupled* noise term on perturbing c_1. $(M = 200, \delta t = 0.1, N_p = 1000)$

Local Sensitivity Analysis - Parameter Perturbation

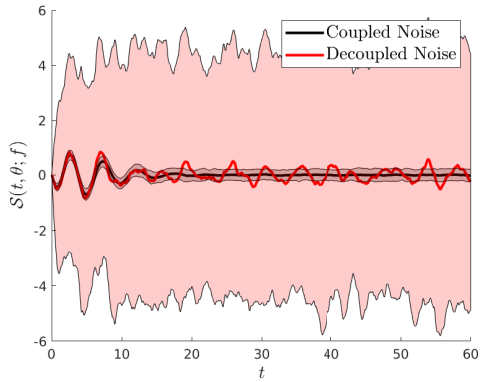

(a) $\mathcal{S}_\varepsilon\left(t, c_1; \mathsf{VAF}\right), M = 10^2$

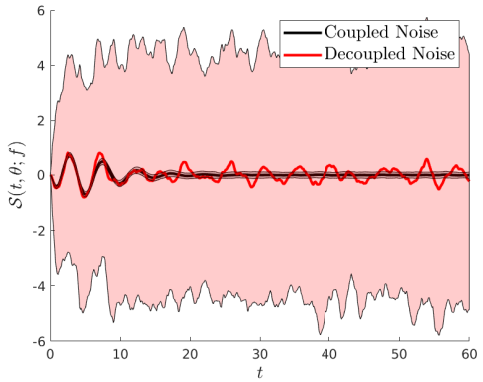

(b) $\mathcal{S}_\varepsilon\left(t, c_3; \mathsf{VAF}\right), M = 10^2$

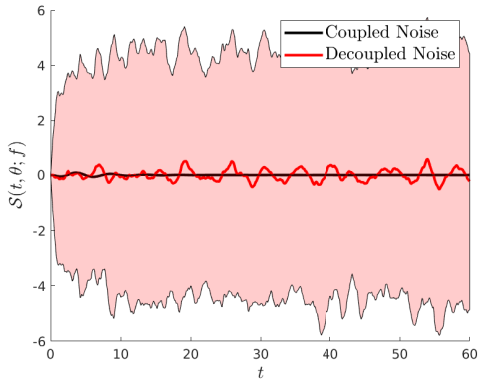

(c) $\mathcal{S}_\varepsilon\left(t, c_6; \mathsf{VAF}\right), M = 10^2$

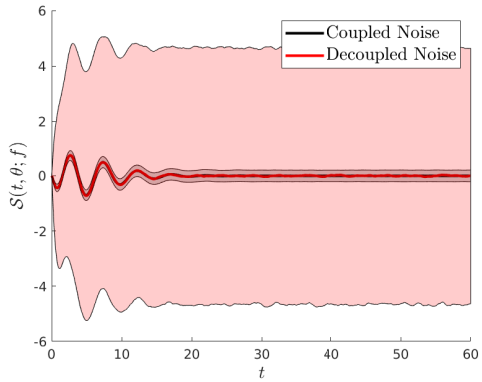

(d) $\mathcal{S}_\varepsilon\left(t, c_1; \mathsf{VAF}\right), M = 10^4$

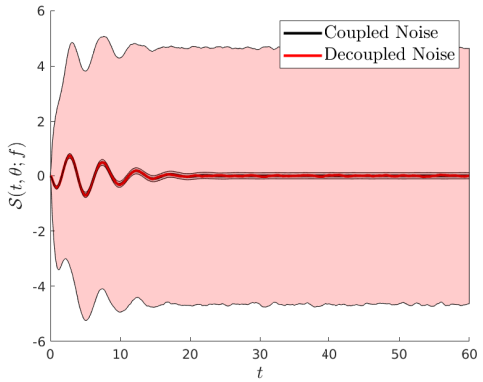

(e) $\mathcal{S}_\varepsilon\left(t, c_3; \mathsf{VAF}\right), M = 10^4$

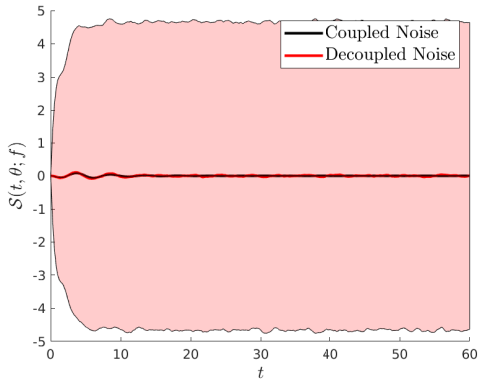

(f) $\mathcal{S}_\varepsilon\left(t, c_6; \mathsf{VAF}\right), M = 10^4$

Figure: Local sensitivity of observable, VAF, due to perturbation of c $\left(\varepsilon = 0.01, \omega_0 = \frac{8}{9}, \mathsf{k_B}T = 10^{-5}\right)$

Global Sensitivity Analysis - No. of Modes Perturbation

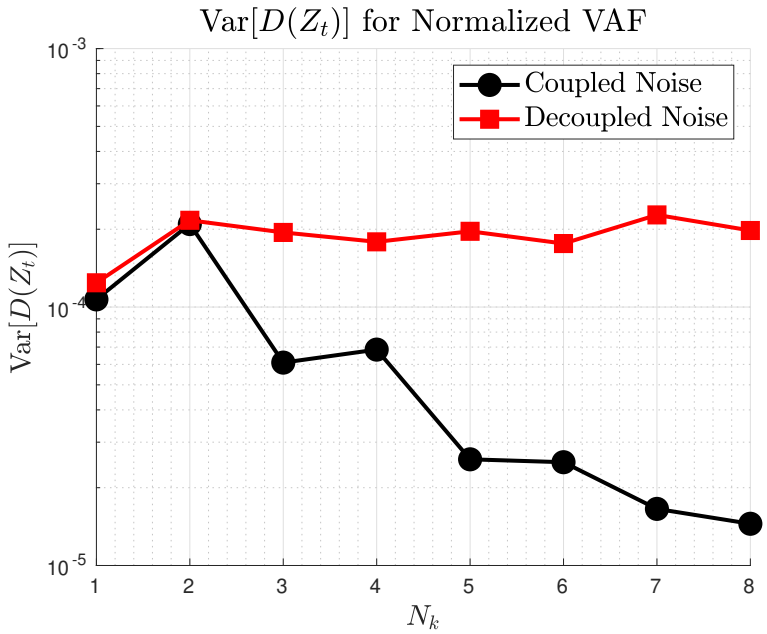

Figure: Var$[D\,(Z_t)]$ where the difference in solution, $D\,(Z_t)$, is between the nominal model with $N_k = n$ and the perturbed model with $N_k = n + 1$ where $n = 1, \cdots, 8$ $(\omega_0 = 8/9, \mathsf{k_B}T = 10^{-5}, t = 100)$.

Though this does not provide a measure for local sensitivity, this provides us information for deciding when we have enough no. of modes in the Prony series approximation of Extended Variable GLE system i.e. the system is no longer sensitive to capture more memory.

Global Sensitivity Analysis - No. of Modes Perturbation

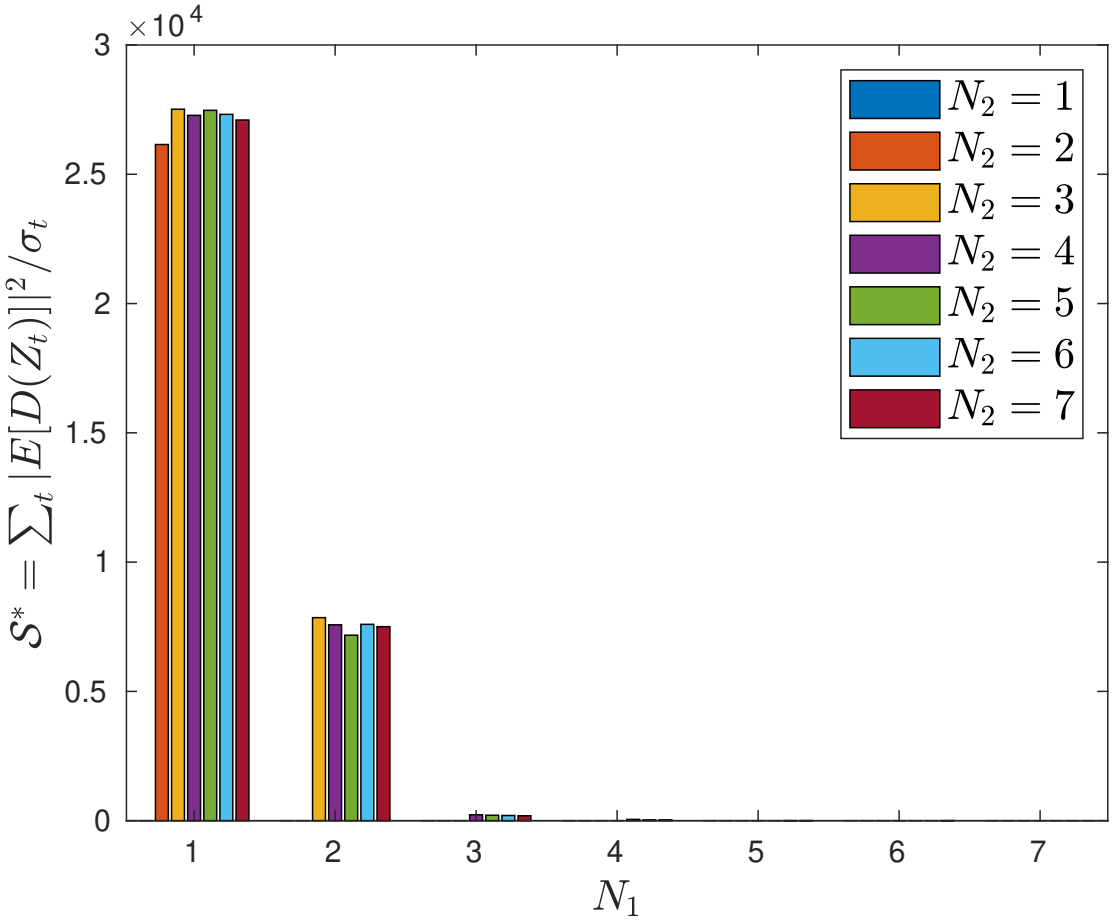

Figure: The global sensitivity index $\mathcal{S}^* = \sum_t \left|\mathbb{E}\left[D\left(Z_t\right)\right]\right|^2 / \sigma_{Z_t}$ gives a quantitative characterization of the difference between the observed VAF on varying the no. of Prony series modes.
$(\omega_0 = 8/9, \mathsf{k_B}T = 10^{-5}, t = 50, M = 10^2)$.

Conclusion

Extended Variable GLE:

- *Non-Markovian* challenge overcome by converting to *Markovian* extended variable GLE problem using Prony series approximation.
- Explicit Euler scheme does not conserve 1^{st} and 2^{nd} moments unlike Splitting scheme.
- Number of modes used in Prony series approximation affects the `memory kernel` fit.

Sensitivity Analysis:

- Significant reduction in variance of the calculated sensitivity on using a common coupled random path for the diffusion term of GLE.
- Order of variance reduction for $D\left(Z_t\right)$ was observed to be $\mathcal{O}\left(\varepsilon^2\right)$ for coupled noise and $\mathcal{O}\left(1\right)$ for decoupled noise.
- Order of variance reduction for Δ_c was observed to be $\mathcal{O}\left(M^{-1}\right)$ for coupled noise and $\mathcal{O}\left(\varepsilon^{-2}M^{-1}\right)$ for decoupled noise.

Outlook

- Parameter fitting over experimental data to see how the noise in the experimental data affects the model.
- Compatibility study of Prony series approximations to other complex potentials.
- Expressing memory kernel in a form such that the problem can be solved using Krylov subspace methods.

References I

Andrew D. Baczewski and Stephen D. Bond.

Numerical integration of the extended variable generalized Langevin equation with a positive Prony representable memory kernel.

Journal of Chemical Physics, 139(4), 2013.

Bruce J. Berne, Jean Pierre Boon, and Stuart A. Rice.

On the calculation of autocorrelation functions of dynamical variables.

The Journal of Chemical Physics, 45(4):1086–1096, 1966.

M. A. Despósito and A. D. Viñales.

Subdiffusive behavior in a trapping potential: Mean square displacement and velocity autocorrelation function.

Physical Review E - Statistical, Nonlinear, and Soft Matter Physics, 80(2):1–7, 2009.

Eric J. Hall, Markos A. Katsoulakis, and Luc Rey-Bellet.

Uncertainty quantification for generalized Langevin dynamics.

Journal of Chemical Physics, 145(22), 2016.

References II

D. J. Higham.

An algorithmic introduction to numerical simulation of stochastic differential equations.

SIAM Review, 43(3):525–546, 2001.

K. Kawasaki.

Simple derivations of generalized linear and nonlinear Langevin equations.

Journal of Physics A: General Physics, 6(9):1289–1295, 1973.

Ben Leimkuhler and Charles Matthews.

Molecular Dynamics.

Springer International Publishing, 2015.

Martin Lysy, Natesh S. Pillai, David B. Hill, M. Gregory Forest, John W.R. Mellnik, Paula A. Vasquez, and Scott A. McKinley.

Model Comparison and Assessment for Single Particle Tracking in Biological Fluids.

Journal of the American Statistical Association, 111(516):1413–1426, 2016.

References III

A. D. Viñales and M. A. Despósito.

Anomalous diffusion: Exact solution of the generalized Langevin equation for harmonically bounded particle.

Physical Review E - Statistical, Nonlinear, and Soft Matter Physics, 73(1):5–8, 2006.